

Assembled Additive Manufacturing – A Hybrid Fabrication Process Inspired by Origami Design

Dongping Deng

Yong Chen*

Daniel J. Epstein Department of Industrial and Systems Engineering
University of Southern California, Los Angeles, CA 90089, U.S.A.

*Corresponding author, Phone: (213) 740-7829, Fax: (213) 740-1120, Email: yongchen@usc.edu

ABSTRACT

Inspired by the recent developments on origami structures, we investigated a fast AM process for fabricating prototype models of thin-shell shapes. By combining the origami design and the additive manufacturing technology, a new fabrication process named Assembled Additive Manufacturing (AAM) is developed. In the process, a digital model is first analyzed to determine geometries that are fabricated by the layer-based and origami-based approaches. The thin shell model for the origami-based approach is then unfolded into a foldable 2D sheet. After the fabrication and folding of the 2D sheet, a postprocessing process is developed before the final prototype is fabricated using the layer-based fabrication process. Algorithms of analyzing and unfolding polygonal model and the details of the process are introduced in the paper; design parameters, mechanics analysis and test cases are also discussed.

KEYWORDS:

Additive manufacturing, in-situ assembly, thin-shell structure, origami design, folding, fabrication speed.

1 INTRODUCTION

Objects with thin-shell structures are commonly used in various products (two product examples are shown in Figure 1a and 1b). Due to the good properties such as lightweight and less used materials, thin-shell structures will be widely used in future engineering systems to satisfy the increasingly important sustainability requirements such as reducing material consumptions. A general method based on offsetting polygonal models was presented to convert a solid object into a hollow one to reduce its weight [1]. A 3D texturing mapping method was also developed for designing complex internal structures to achieve both lightweight and required strength [2]. Two hollow structure examples are shown in Figure 1c and 1d.

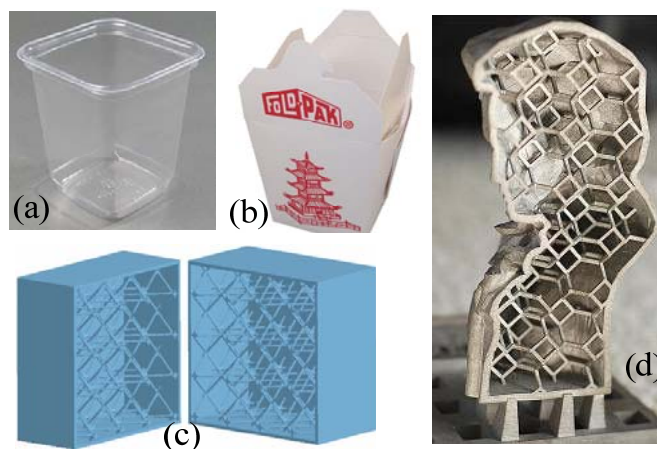


Figure 1: A hollow structure example [2].

Hollow objects with thin-shell structures are usually difficult to be fabricated by the subtractive- or deformation-based manufacturing processes (e.g. machining and injection molding) due to the difficulty for tools to access the internal features. In comparison, the layer-based additive manufacturing (AM) processes can overcome such accessibility limitations by converting a 3D model into a set of 2D layers for its fabrication [3, 4]. Hence, the AM processes seem more suitable for the fabrication of hollow objects with thin-shell structures.

A large thin-shell feature usually requires a large number of layers in the AM processes. However, the fabrication efficiency of each layer is not high since only a small amount of material is accumulated in each layer for such thin-shell features. In recent years, a paper folding art named *origami* has attracted increasing attentions. The origami design is to study how a 2D paper can be folded into a 3D structure [5]. Such a folding-based approach can potentially be a simple and fast method to create hollow objects with thin-shell structures. Various issues such as the crease design and folding sequence have been studied in the origami design [6-8].

Inspired by the recent developments on the origami design, a new AM process named *Assembled Additive Manufacturing* (AAM) was developed. The key idea of the AAM process is to integrate the layer-based fabrication approach with appropriate folding operations to significantly improve the fabrication speed. Hence the AAM process is a hybrid fabrication method by integrating both folding and layer-based fabrication approaches.

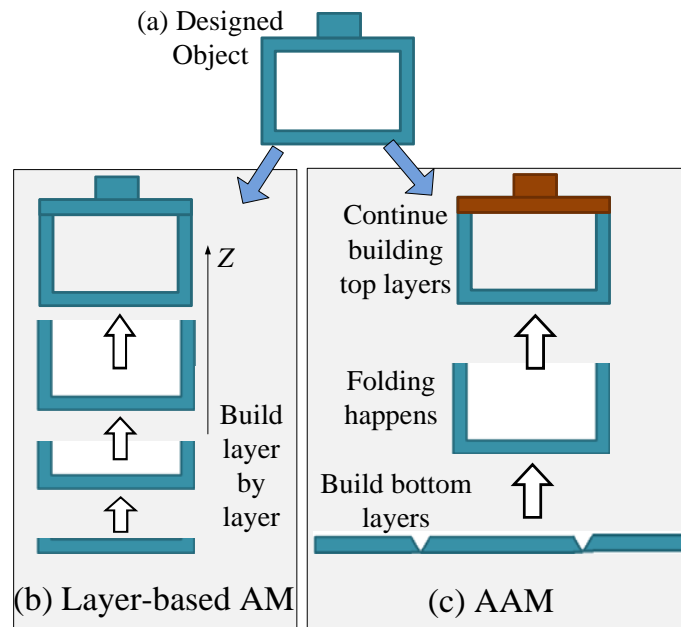


Figure 2: An illustration of the AAM process versus the traditional layer-based AM processes.

Figure 2 shows an illustration example to compare the AAM and the traditional layer-based AM processes. Suppose a computer-aided design (CAD) model with thin-shell structures is given (refer to Figure 2a). Based on it, the fabricating process based on the layer-based AM approach is shown in Figure 2b. Note that there may be hundreds of layers in building the middle thin shell portion. In comparison, the AAM process uses a hybrid fabrication approach, which is shown in Figure 2c. First, an unfolded structure is fabricated by the layer-based fabrication approach; the fabricated 2D structure is then folded into a 3D structure in a single operation; finally, the layer-based approach is used to continue the fabrication of the remaining top portion. Due to the folding operation, the required building layers can be significantly reduced. Consequently, the AAM process can speed up the fabrication of such hollow objects.

2 ASSEMBLED ADDITIVE MANUFACTURING PROCESS

The AAM process integrates the folding and the layer-based fabrication process. An unfolded 2D structure includes designed creases and 2D thin-shell structures. Both of them can be fabricated using the layer-based AM processes. The folding of the fabricated 2D thin-shell structures can be applied during the AM fabrication process or after completing the AM fabrication process. Both scenarios are demonstrated in the paper. In addition, multiple materials may be required in the AAM process in order for the creases and 2D thin-shell structures to be properly folded.

Various AM processes can be used in fabricating 2D origami sheets and other 3D features in the AAM process. In this paper, the AM process that is used for demonstrating the AAM process is the *mask-image-projection-based stereolithography* (MIP-SL) process [9, 10]. In the process, a mask image is dynamically defined by a *digital micromirror device* (DMD). A DMD is a *micro-electro-mechanical system* (MEMS) device that enables one to simultaneously control over 1 million small mirrors. Accordingly a pixel can be turned on or off at over 5 KHz. Using the technology, the energy input related to a mask image can be provided in solidifying a layer of photo-curable resin.

Figure 3 shows a bottom-up projection based MIP-SL process. In our study, it is used as the experimental setup of the AAM process. In the building process, a mask image is projected at the bottom of the resin tank. A layer of photocurable resin is cured into the shape defined by the related image. Using a two-way movement method [11], the cured layer can be detached from the coated tank to enable the Z-stage to move up a small distance related to a given layer thickness. Since a mask image can simultaneously cure a whole layer of the resin, the MIP-SL process can fabricate a large 2D origami sheet defined in the AAM process quickly.

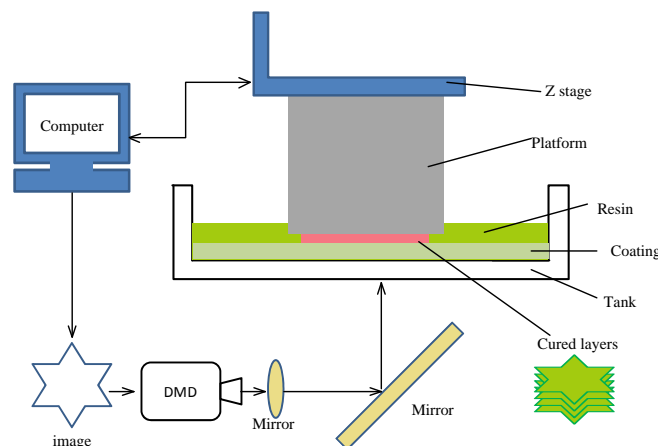


Figure 3: An illustration of the MIP-SL process.

In the AAM process, the foldable portions of a given 3D model need to be identified first. Based on them, appropriate 2D origami structures will be designed. In addition, appropriate folding actions will be planned in the model fabrication process. Note, in the origami design (e.g. [12]), all the 3D structures are required to be built by folding a single 2D origami sheet; in comparison, in the AAM process, only portion of geometric features will be built by the folding mechanism. Other geometric features that are hard to be folded will still be fabricated by the layer-based AM process.

A 3D model can be decomposed in many different ways for analyzing foldable portions, e.g. by the cellular decomposition, or by direct analysis of a polygonal model. For a given geometry, some portions of a polyhedron may be easily unfolded into a 2D origami structure with small approximation errors. However, it may be difficult to unfold some other geometric features. For example, in a simple test case as shown in Figure 4, the green portion of the object may be easily fabricated through the folding operation; however, the gray portions on the top and bottom of the green cube are difficult to be unfolded. Instead the two cylinders can easily be built using the layer-based fabrication approach. Hence a detection algorithm is required to decompose a given 3D model into foldable and unfoldable regions.

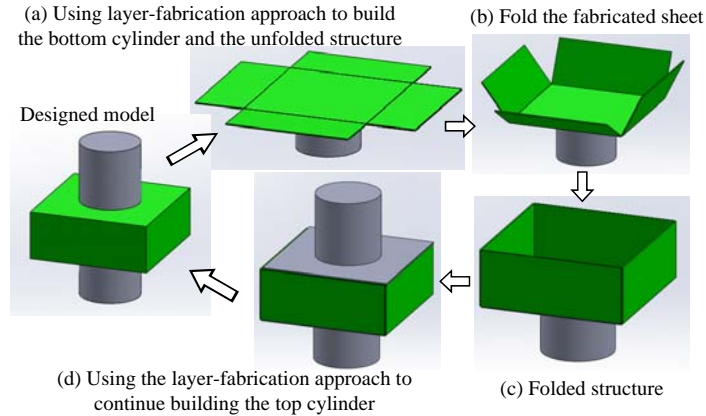


Figure 4: An example of the AAM process.

The feature-based model decomposition approaches have been studied before. However, such approaches are generally knowledge-based and not general. Based on the decomposition of the CAD model as shown in Figure 4a, the AMM fabrication process for the model is shown in Figure 4b-4d. In general, the AAM process needs four main steps as shown in Figure 5: (1) An approximation algorithm is used to convert a given CAD model into a foldable model representation; (2) an unfolding algorithm is used to unfold the approximated model into a 2D origami sheet structure. Appropriate crease structures are required to be added in the origami structure as well; (3) the 2D origami sheet structure is fabricated and folded into a 3D object; and (4) a post-processing step is applied to the folded structure to bond the creases and to add additional structures if needed.

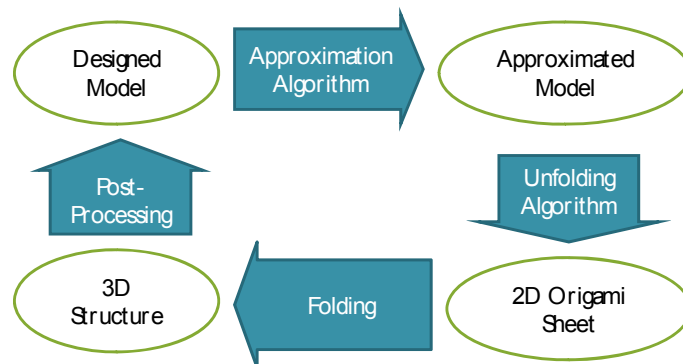


Figure 5: Main steps of the AAM process.

Two critical issues in the AAM process include: (i) how to convert a thin-shell structure into a foldable 2D structure; and (2) how to fold a 2D structure into a designed 3D shape. Our study on the issues is discussed in the paper and the remainder of the paper is organized as follows. An unfolding method based on the cellular and CSG decomposition is discussed in Section 3. A foldable structure design is presented in Section 4. The folding mechanism including the angle control is presented in Section 5. Some experimental results of the AAM process are presented in Section 6. A fabrication speed comparison between the AAM and traditional layer-based AM processes is also given in Section 6. Finally conclusions are drawn in Section 7 with some future work.

3 UNFOLDING OF A CAD MODEL

A given 3D model can have infinite number of solutions when unfolding it into a 2D sheet. A general decomposition and folding method is desired for a given CAD model. A cellular-based decomposition method is developed for the AAM process including two main steps, (1) approximating a 3D model with a set of voxels, and (2) the unfolding of the voxels into a 2D sheet.

3.1 Approximation of a 3D Model

Folding a 2D sheet can only generate a polyhedron with flat surfaces. To better utilize the folding process, it is desired to simplify a given 3D model by removing curved surfaces. In addition, a simple geometric representation is preferred in defining and analyzing the given geometry.

To unfold a given CAD model, an approximation step is first applied to generate a simpler representation of the 3D model. Two choices have been considered in such an approximation step. The first approximation method is the voxelization by converting a given 3D model into a set of voxels. The second approximation method is based on the Constructive Solid Geometry (CSG) representation by converting a given 3D model into the Boolean results of some CSG primitives [13]. Both approximation methods can lead to a simpler model that is easier to be analyzed. In comparison, (1) the voxelization provides a simple and general approach for any given geometry. The accuracy of the method is related to the resolution of the voxels. The higher the resolution, the better approximation the generated voxels will have. However, the related unfolding and folding process will be more complex. (2) The CSG approximation can use less primitive to capture the original geometry. Consequently, the related folding process can be simpler. However, the decomposition of a complex geometry may require significant efforts since it is difficult to have a general method. Both decomposition methods have been investigated for the AAM process. They are discussed as follows.

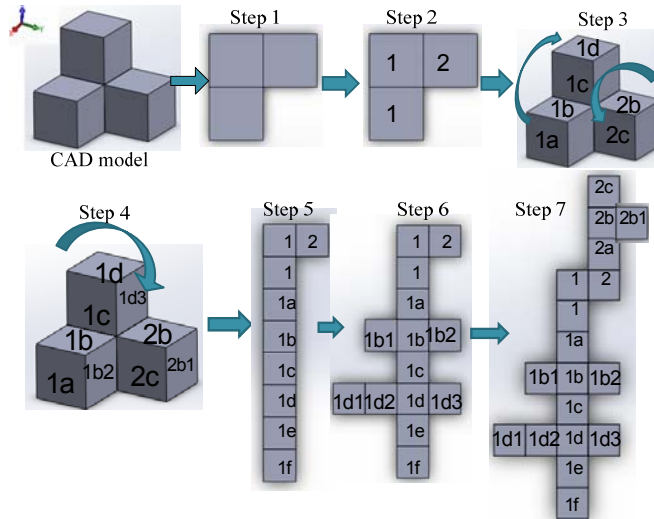


Figure 6: An unfolding algorithm for a voxel-based model.

3.2 Unfolding algorithms for voxels and CSG models

Based on the two aforementioned approximation methods, the unfolding of a 3D model can be classified as the voxel-based and the CSG-based approaches.

(1) For a voxel-based model, several algorithms can be used to unfold the voxel representation into a 2D origami sheet. Figure 6 shows a simple example. Suppose a 3D model is approximated by four voxels, which are used to define the input geometry. Note that a voxel model has only flat surfaces with fixed folding angles. Consequently the unfolding problem for voxels can be simplified. As shown in Figure 6, (1) suppose the bottom surface is set as the 2D plane in the unfolding process. (2) The bottom units are labeled based on their columns: the case as shown in Figure 6 has only two columns: 1 and 2. (3) The faces on each column are labeled in a specified orientation as a loop: for example, the faces in column 1 are labeled in the clockwise orientation as $1a$, $1b$, $1c$, etc. The faces in column 2 are labeled in a reverse orientation as $2a$, $2b$, etc. (4) For each labeled column face, its neighboring faces in the same column that have not been labeled will be marked as its child faces: for example, the child faces of $1d$ are marked as $1d1$, $1d2$, and $1d3$. In addition, the child face $1d3$ is linked to the face $2b$ in column 2. (5) The faces of one column can be unfolded in the sequence based on their labels. (6) The child faces of each column face

can be unfolded and added to its neighbors. (7) Similarly, the next column can be processed until all the columns have been unfolded.

(2) For a CSG-based model, each basic primitive can be unfolded separately. The unfolded structures can then be assembled based the Boolean operations that are performed between the primitives of the CSG model. Figure 7 shows an example. The designed model can be decomposed into two primitives, a cube and a triangular prism. The unfolded structures of the two primitives are shown in the figure. The Boolean operation between the two primitives is a *Union* operation. Based on it, a final origami sheet can be assembled based on the topological relations of the two unfolded surfaces (i.e. faces 1 and 3 are neighboring faces).

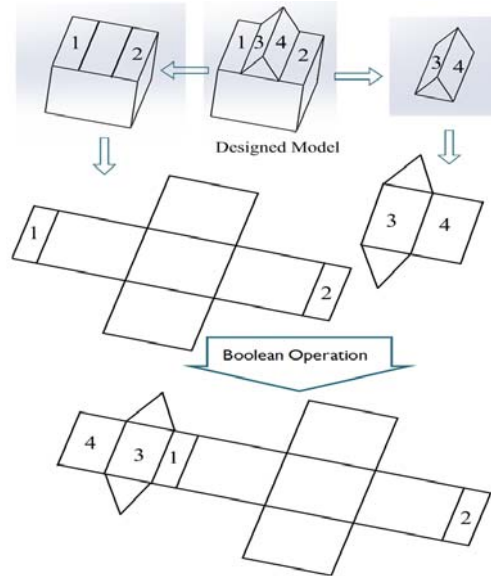


Figure 7: An unfolding algorithm for a CSG-based model.

4 FOLDING OF 2D ORIGAMI SHEET

Appropriate crease structures need to be designed in order for a 2D origami sheet to be foldable. The MIP-SL process can easily fabricate multi-layer structures with complex geometry in each layer. In addition, multiple types of materials can be added in the MIP-SL process [14]. In our study, three types of crease structures have been tested. One is based on a multi-material crease design, and the other two structures are based on different geometric designs using a single material.

4.1 Foldable crease designs

For a 2D origami sheet that is unfolded from a 3D model, the designed creases can have either a soft material or a specially designed geometry to make it foldable.

(1) To fabricate a foldable 2D structure, a multi-material-based crease design is shown in Figure 8. In the crease model, a soft material is used to enable the folding along the crease while a rigid material is used in the other portions to achieve a better structural property. The fabricated physical model is shown in Figure 8b. The soft portion is shown in transparent, which connects two hard portions in both sides (as shown in yellow). Hence the crease can be folded to a certain angle. Figure 8c shows a fabricated origami sheet structure by unfolding a box.

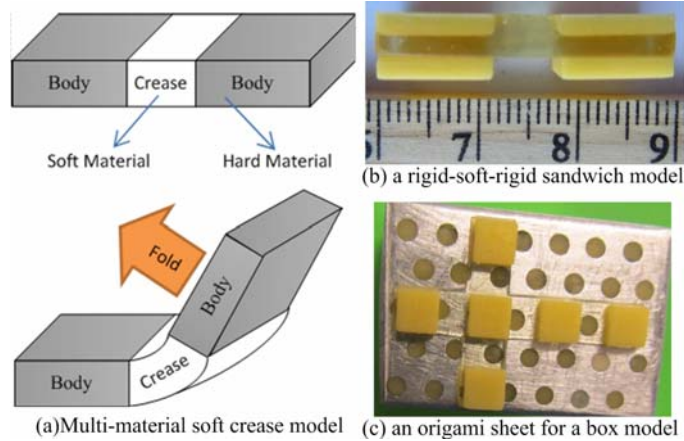


Figure 8: A multi-material soft crease design and its samples.

(2) Two hinge designs based on a rigid material are shown in Figure 9. Figure 9a shows a living hinge structure design. Such a hinge structure has been widely used in various polymer-based lid designs. The hinge can be folded because it has a relatively thin feature in its crease. The relative dimensions of the specific living hinge design will make the structure sufficiently flexible to be folded and unfolded. Another hinge design based on a pattern structure is shown in Figure 9b. The crease portion uses a pre-defined pattern such that the hinge can be flexible and the related structure can be folded and unfolded. The built physical objects based on the two hinge designs are also shown in the figure.

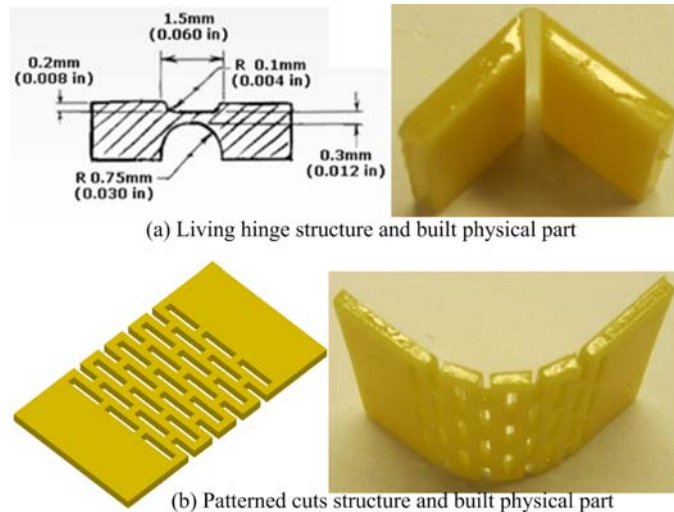


Figure 9: Two foldable hinge designs based on a single material. (a) A living hinge structure design; and (b) a pattern structure based hinge design.

4.2 A comparison of the three crease designs

Based on our tests, the multi-material-based crease design and the two single-material-based hinge designs can all realize the folding operation of a 2D origami sheet. Table 1 presents the advantages and disadvantages of the three crease designs.

For the AAM process, (1) the multi-material-based soft crease has good strength and large bending angle. However, the crease is relatively bulky. In addition, the fabrication process is more complex since two types of materials are required in building the crease model. (2) The single-material-based living hinge structure is simple, compact, and can achieve a large bending angle as well. However, the structure is relatively weak and easy to be torn due to the thin hinge connection. (3) The pattern structure based hinge model has good strength. However, the structure is bulky and only has a limited bending angle.

Table 1: A comparison of three foldable crease designs.

Model type	Advantages	Disadvantages
Soft crease	Good strength; flexible bending angle	Bulky, two materials
Living hinge	Simple; one material; Space saving Flexible bending angle	Weak connection
Patterned cuts	Modest strength; one material	Bulky, bending angle limited

The choice of an appropriate crease design depends on the 2D origami sheet design, the folding angle of a crease, and the capability of the AM processes. For the MIP-SL based AAM process, the single-material-based living hinge design is selected in building the test cases as discussed in Section 6.

5 FOLDING ACTUATION AND CONTROL

Another important issue in the AAM process is the folding actuation and the accurate folding angle control. An aforementioned crease design can be folded using either internal or external actuation mechanisms. An internal actuation mechanism means the 2D structure can be folded by some embedded actuators such as a shape memory alloy foil or a shape changeable film. An external actuation mechanism means the structure is folded using some external forces such as robotic hands or some specially designed folding devices. Both internal and external actuation mechanisms have been tested in our study. The test results demonstrate that both approaches can be used in the AAM process.

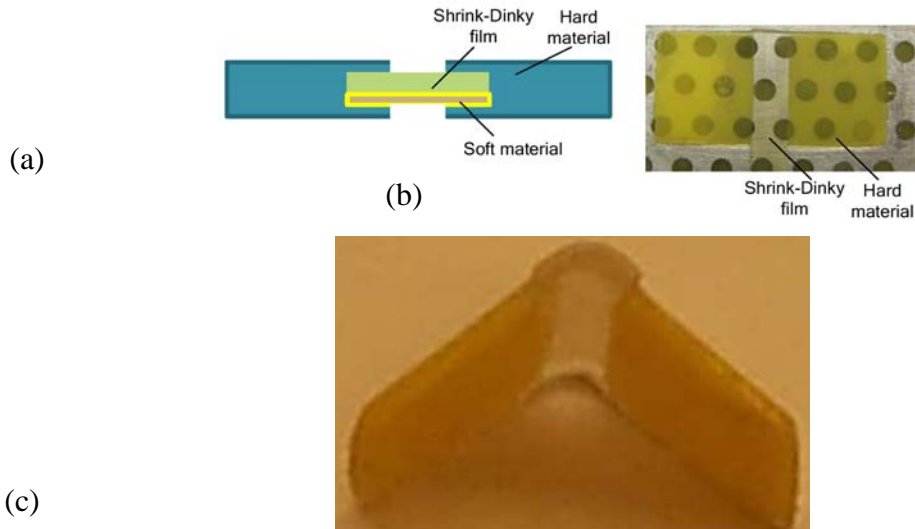


Figure 10: A polystyrene film embedded in a multi-material crease design. (a) A PS film based design; (b) a built physical model; and (c) a self-folded structure after heating.

5.1 A plastic film based actuation mechanism

To demonstrate the internal actuation approach, a polystyrene (PS) plastic film is embedded in the designed crease structures. The selected PS film is thermally sensitive and will quickly shrink over 30% when temperature overpasses a transition temperature ($\sim 120^{\circ}\text{C}$). A multi-material soft crease with an embedded PS film is shown in Figure 10. The film is constrained by the rigid material in both sides of the crease. In addition, a soft material is used to cover the bottom of the PS film. Hence the PS film is only

exposed to the outside environment from the top side. Consequently, when such a crease is exposed to a heated environment, the top side will shrink while the bottom side is constrained by the soft material. The one-side shrinkage of the PS film will generate a bending movement of the designed crease. A fabricated crease structure based on the MIP-SL process is shown in Figure 10b. After putting the 2D origami structure in a pre-heated oven with a temperature over 120°C, the crease will be bended to a folding angle around 90° in less than 10 seconds (refer to Figure 10c).

The PS film can also be embedded in a single-material-based structure design as shown in Figure 11a. The PS film is indicated in green color. It is sandwiched by rigid material (in yellow) in both sides. However, in the crease portion, only one side of the film is covered by the rigid material while the other side is exposed to the outside environment. When the structure is heated, the one-side shrinkage of the PS film will bend the crease towards the side that is exposed to the heated air. Figure 11b shows a fabricated origami sheet structure for an open box model. When the structure is put in a pre-heated oven with a temperature over 120°C, the structure will fold into a structure as shown in Figure 11c in around 10 seconds. The detail analysis of the bending effect and related parameter settings for desired bending angles will be presented in other publications.

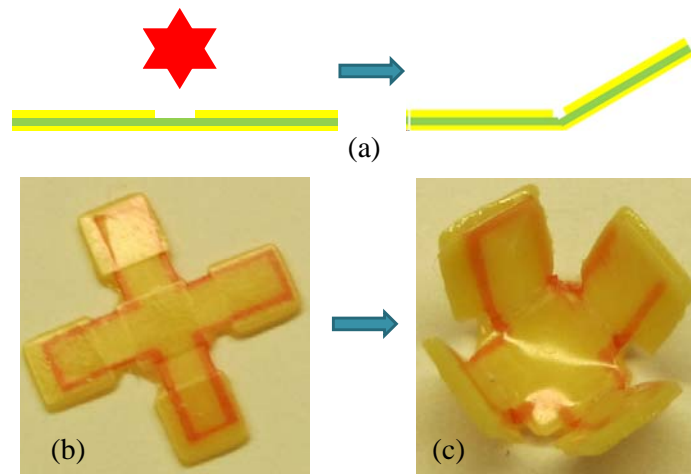


Figure 11: A polystyrene film embedded in a single-material crease design. (a) A PS film based design; (b) a built physical model – the embedded PS film is highlighted in red; and (c) a self-folded structure after heating.

5.2 An external actuation mechanism

An external actuation approach based on manual operations has been tested. Manual operations, although being slow, can easily fold complex crease structures. In the future, robotic hands or specially designed actuation devices can be developed to replace the manual operations such that the folding process can be automatic. The development of such actuation devices needs to consider three main issues including: (1) the separation of a folding portion from its constraints; (2) determining the holding position of a crease during the folding process; and (3) designing required folding motions that have no collisions. For a single crease, the development of such an actuation device is straightforward; however, the actuation devices can be complex when multiple hinges in a 2D origami sheet need to be folded by following a certain sequence. The development of such actuation devices for the AAM process will be studied in our future work.

5.3 An angle lock design

To achieve a controlled bending angle, an angle lock design has been developed for the living hinge design. As shown in Figure 12, two angle fixtures are added in the both sides of the crease. Based on them, the bending angle can be accurately controlled through their geometrical relationship. In addition, the friction between the angle fixture 1 and 2 can fix the folded structure as well.

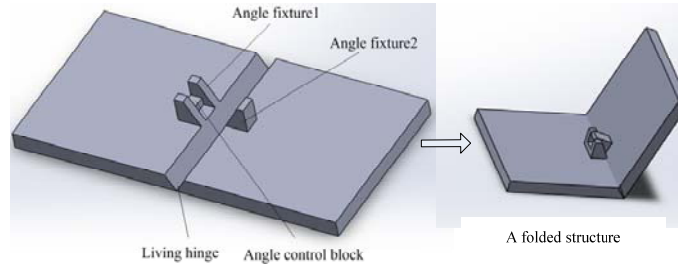


Figure 12: An angle lock design

Figure 13 shows a built test case with the angle lock design. The structure is manually folded and could be firmly fixed through the friction between the two angle fixtures. Two or more angle fixtures can also be added in the crease to ensure the folded structure to be securely fixed in the designed angle.

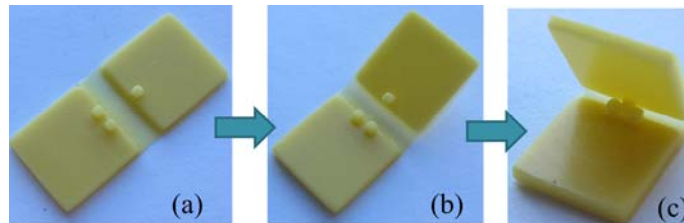


Figure 13: A built structure with angle lock design.

After the built 2D origami sheets are folded into 3D structures, the last step in the AAM process is the post-processing of the folded creases. In this optional step, additional liquid resin can be added to the creases and then be cured by external light sources such as a projector or a portable LED light [15]. Consequently, the two sides of the creases can be permanently bonded by the added cured resin.

6 TEST CASES

Two types of test cases are designed for physical experiments including folding during and after the layer-based fabrication process. In the first type, three test cases are designed, which are shown in Figures 14 and 15. In the tests, only certain portions of the models are fabricated by the folding approach; the other portions are fabricated by the layer-based AM approach. In the second type, another three test cases are designed, which are shown in Figures 16 and 17. In the tests, the folding operations are used after the whole origami structures have been fabricated by the MIP-SL process. In addition, the fabrication speeds of the AAM and layer-based AM processes are compared for the six test cases.

7.1 Test cases using a hybrid fabrication approach

Figure 14a shows a designed CAD model to be fabricated by the AAM process. The input model is decomposed into two portions, a foldable thin-shell structure and a top lid. Accordingly the building process based on the decomposed portions is shown in Figure 14b. An unfolded 2D sheet with designed creases based on living hinge structures is fabricated. The portions that need to be folded are detached from the platform while the other portions remain on the platform. The folding of the detached 2D structures is realized through manual operations. After the 2D structure is folded into the desired 3D structure, the MIP-SL process will resume until the remaining top layers are finished. Finally the built object will be taken out from the platform for cleaning. Figure 14b shows the built object using the AAM process.

Based on a similar building process, foldable structures with more complex features can be fabricated. Two test cases with additional features on the side surfaces are shown in Figure 15. Note that such features can be easily built in the XY plane while it is difficult to fabricate them in the Z axis due to the issues such as over-curing in the Z axis and additional supports in the MIP-SL process. The added supports may also be inside a hollow object and hence will not be easily removed. In comparison, such

features on the side surfaces can be unfolded to the bottom surface in the AAM process (refer to Figure 15b). After the 2D surfaces in the XY plane have been built, the side surfaces can be folded into a 3D structure. Figure 15c and 15d show the fabricated 3D objects.

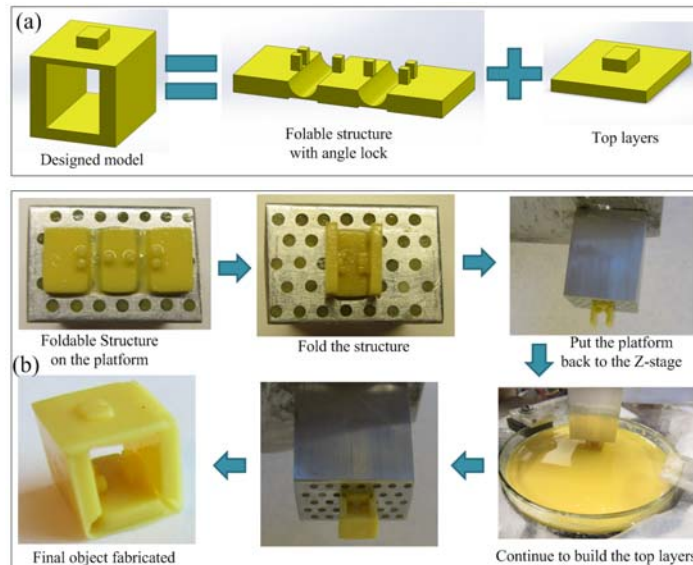


Figure 14: Fabrication procedure of the AAM process.

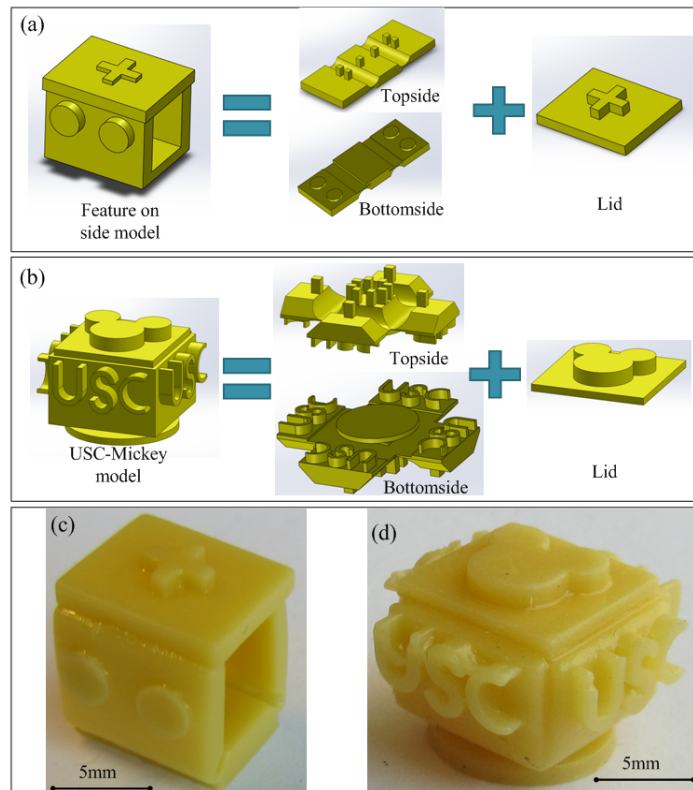


Figure 15: Two test models.

Note that the USC-Mickey model as shown in Figure 15d is hollow with a fully enclosed volume. Other manufacturing processes will not be able to build such a hollow object since tools will not have access paths to its internal features.

7.2 Test cases using folding after AM fabrication

Figure 16 shows a simple test case based on the folding operations after the MIP-SL process. For a given box model, a foldable origami sheet is designed with the living hinges added to all the creases. The unfolded 2D structure is fabricated. It is then manually folded into a 3D structure. The folding operations need to be controlled to avoid breaking the hinge structures. A tape can be used in temporarily fixing the folded structure. In the test, a small amount of liquid resin is added to the folded creases. The resin is then cured by a hand-held light source. After removing the tape, the fabricated box is also shown in Figure 16. The top lid can easily be opened and closed.

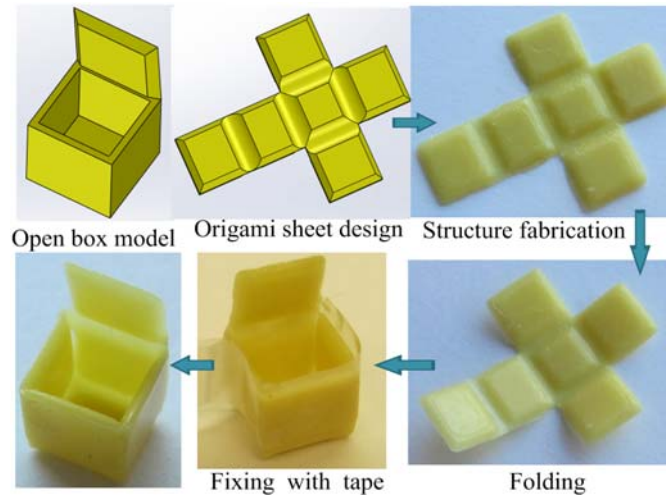


Figure 16: A test case of an open box model.

Figure 17 shows two more test cases. Similar to the test cases as shown in Figure 15, some additional features can be added to the side surfaces. Such features can easily be built in the XY plane by the MIP-SL process. The built features can then be folded into planes with desired angles, e.g. 90° in Figure 17a and 60° in Figure 17b.

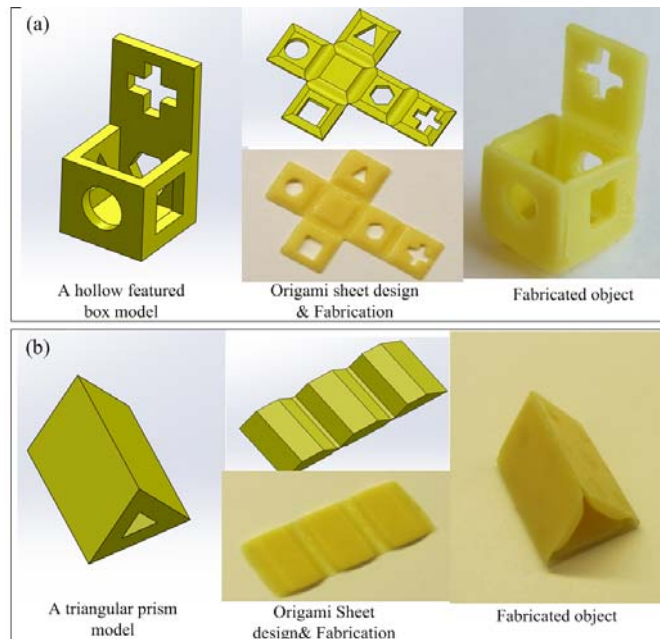


Figure 17: Two test cases. (a) A hollow box model; and (b) a triangular prism model.

7.3 Fabrication speed analysis

The AAM process can reduce the fabrication time by converting 3D features that requires the Z axis fabrication process into an unfolded 2D features that requires the fabrication of a single XY plane. Hence the required number of layers can be significantly reduced.

Table 2 show a fabrication speed analysis of the six aforementioned test cases for the AAM process. The manual operation time has been considered in the building time analysis. The folding of the creases will typically take less than 2 to 3 minutes depending on the operator’s experience. For a comparison, the fabrication time of the layer-based AM processes is also shown in the table. In the analysis, it is assumed that the AM process will take 30 seconds in building a layer. Thus the layer number will directly affect the fabrication time. As shown in the table, the AAM process can significantly reduce the fabrication time for the tested thin-shell structures.

Table 2: A comparison between the AAM and AM processes on the fabrication speed.

MODEL						
AAM Fabrication Layer Num.	27+15 -42	36+15 -51	46+14 -60	9	7	13
AM Fabrication Layer Num.	95	102	98	60	128	70
AAM Fabrication Manual operation	3min	3min	3.5min	2min	2min	1.5min
AAM Fabrication Total Time	24min	28.5min	33.5min	6.5min	5.5min	8min
AM Fabrication Total Time	47.5min	51min	49min	30min	64min	35min
Saved time ratio	49.5%	44.1%	31.6%	78.3%	91.4%	77.1%

7 CONCLUSION AND FUTURE WORK

In the paper, an origami inspired additive manufacturing process named *Assembled Additive Manufacturing* (AAM) has been developed. The main idea of the AAM process is to integrate the folding based fabrication process with the layer-based fabrication process. Some general issues related to the AAM process are discussed including the approximation of a CAD model, unfolding of a 3D model, the design of foldable structures and related folding mechanisms. Experimental tests of the AAM process have been performed to compare the fabrication speeds of the AAM and the layer-based AM processes. Some potential benefits of the AAM process have been demonstrated for hollow objects including shortening the fabrication time and removing the needs of supports.

A significant amount of work remains in order to mature the newly developed AAM process. Some future work includes (1) developing a more general unfolding algorithm for a given CAD model; (2) developing internal and external actuation mechanisms for a better control of the self-folding and automatic folding; (3) testing the AAM process in the micro-scale size level; and (4) identifying novel applications of the AAM process.

ACKNOWLEDGEMENTS

This work is partially supported by National Science Foundation CMMI-1151191.

REFERENCES

- [1] Chen, Y., C. C. L. Wang (2011). Uniform offsetting of polygonal model based on Layered Depth-Normal Images. *Computer-aided design*, Vol. 43, No. 1, pp.31-46.
- [2] Chen, Y. (2007). 3D texture mapping for rapid manufacturing. *Computer-aided design and application*, Vol. 4, No. 6, pp. 761-771.
- [3] Gibson, I., Rosen, D. W., Stucker, B. (2010). *Additive manufacturing technologies: Rapid prototyping to direct digital manufacturing*. New York; London: Springer. doi: 10.1007/978-1-4419-1120-9.
- [4] Kaufui V. Wong, and Aldo Hernandez. (2012). A review of additive manufacturing. *ISRN Mechanical Engineering*, doi: 10.5402/2012/208760.
- [5] Demaine, E. D. (2006). *Origami, linkages, and polyhedra: Folding with algorithms*. (pp. 1-1). Berlin, Heidelberg: Springer Berlin Heidelberg. doi: 10.1007/11841036_1.
- [6] Lang, R. (1996). A computational algorithm for origami design. 98-105. doi: 10.1145/237218.237249.
- [7] Ionov, L. (2011). Soft microorigami: Self-folding polymer films. *Soft Matter*, doi: 10.1039/c1sm05476g.
- [8] Liu, Y., Boyles, J. K., Genzer, J., & Dickey, M. D. (2012). Self-folding of polymer sheets using local light absorption. *Electronic supplementary information (ESI) available*.
- [9] Zhou, C., Chen, Y., and Waltz, R. A. (2009). Optimized mask image projection for solid freeform fabrication. *Journal of Manufacturing Science and Engineering*, 131(6).
- [10] Zhou, C., and Chen, Y. (2012). Additive manufacturing based on optimized mask video projection for improved accuracy and resolution. *SME Journal of Manufacturing Processes*, Vol. 14, No. 2, pp. 107-118.
- [11] Pan, Y., Zhou, C., Chen, Y. (2012). A fast mask projection Stereolithography process for fabricating digital models in minutes. *ASME Journal of Manufacturing Science and Engineering*, Vol. 134, No. 5, pp. 051011.
- [12] Demaine, E. D., and O'Rourke, J. (2007). *Geometric Folding Algorithms: Linkages, Origami, Polyhedra*. Cambridge University Press.
- [13] Saxena, A., and Sahay, B. (2005). *Solid modeling*. Springer. doi: 10.1007/1-4020-3871-2_8.
- [14] Zhou, C., Chen, Y., Yang, Z., Khoshnevis, B. (2013) Digital material fabrication using mask-image-projection-based Stereolithography. *Rapid Prototyping Journal*, Vol. 19, No. 3.
- [15] Chen, Y., Zhou, C., Lao, J. (2011). A layerless additive manufacturing process based on CNC accumulation. *Rapid Prototyping Journal*, Vol. 17, No. 3, pp. 218-227.